

Short Communication

# Electrochemical Oxidation Treatment of Municipal Solid Waste Landfill Leachate Using Pt Nanoparticles Modified Boron-Doped Diamond Electrode

Yaguang Zhao<sup>1</sup>, Xianying Zhao<sup>2,\*</sup>

<sup>1</sup> School of Environmental and Municipal Engineering, North China University of Water Resources and Electric Power, Zhengzhou 450045, China

<sup>2</sup> Zhengzhou Jize Environmental Protection Technology Co. LTD, Zhengzhou 450007, China

\*E-mail: [rain\\_8880583@sina.com](mailto:rain_8880583@sina.com)

Received: 25 December 2020 / Accepted: 6 February 2021 / Published: 28 February 2021

---

This study focused on treatment of municipal solid waste landfill leachate on boron-doped diamond (BDD) and Pt nanoparticles modified BDD (Pt NPs/BDD) by electrochemical oxidation process. The BDD anode was synthesized using MWCVD technique and Pt nanoparticles were electrodeposited on prepared BDD electrodes. The properties of prepared BDD and Pt NPs/BDD anodes were analyzed by SEM, XRD, Raman and electrochemical analyses. The SEM and XRD characterizations showed that the homogeneous and dense diamond crystals covered the both electrode surfaces and for Pt NPs/BDD electrodes, Pt nanoparticles in fcc crystal phase scattered over the BDD surface. Raman analysis indicated to presence of non-diamond carbon impurities in BDD structure and higher degree of lattice imperfections because of the incorporated Pt particles in Pt NPs/BDD structures. The electrochemical oxidation measurements showed that chemical oxygen demand (COD) was decreased about 67.8 %, 69.0 % and 71.8 % on BDD, and decreased about 76.4 %, 84.3 % and 91.9 % on Pt NPs/BDD for current densities of 15, 50 and 100 mA cm<sup>-2</sup>, respectively, after 5.5 hours treatment. Results show that Pt NPs/BDD had the most efficiency to remove COD by electrochemical oxidation process. Scattered Pt nanoparticles on BDD could promote the electrochemical oxidation rate of organic pollutants through the enhancement of the physically adsorbed hydroxyl radicals and chemisorbed oxygen in metal lattice. Thus, there were more oxidation states on the active surface of Pt NPs/BDD electrodes and more adsorbed hydroxyl radicals interacted with BDD surface. Therefore, Pt NPs/BDD in this study provided the synergetic effect of BDD and Pt advantages to electrochemical oxidation of COD.

---

**Keywords:** Electrochemical oxidation; Treatment; Landfill leachate; Pt nanoparticles, BDD

## 1. INTRODUCTION

Landfill leachates derived from municipal landfill wastes are extremely contaminated that the changes in physical, chemical, and biological properties can lead to non-avoidable heavily toxicity in soil, agricultural products, and sources of water and water supply systems due to leachate's migration

through refuse and reverse osmosis process[1]. Moreover, municipal landfill wastes can release the pollutants through biogas, incineration plants, *waste composting*, and transfer systems [2].

Landfill leachates generally contain hazardous organic and inorganic contaminants, xenobiotics, ammonia nitrogen pollutants, toxic complex substances and various heavy metals [2, 3]. On the other hand, development in industrial activities, growth of population, and change in lifestyle are the main reasons for exponential generation of landfill leachates over the years [3, 4]. Therefore, prevailing waste management strategies, pollution control and treatments are the big challenges in world-wide[5, 6]. Accordingly, design and study of treatment systems to obtain the appropriate removal of pollutants is necessary[7]. In last decades, Biodegradation, chemical oxidation, photocatalysis, coagulation–flocculation, ion exchange, chemical precipitation, stripping, ozonation, membrane processes, activated carbon adsorption, electro-Fenton, and electrochemical oxidation are the more applicant techniques to treatment of landfill leachates [8-12]. Among them, electrochemical oxidation as treatment methods could remarkably remove concentrations of leachate organic contaminants such as biochemical oxygen demand (BOD) and COD.

BDD as interest anode can weakly interact and form strongest oxidants such as physisorbed hydroxyl radicals which lead to decomposition or oxidation of organic matter into easily available forms to plants. Therefore, BDD is a noteworthy non-active anode to performance of treatment of wastewater containing leachate contaminants [13]. Therefore, this study presented treatment of municipal solid waste landfill leachate BDD and Pt NPs/BDD by electrochemical oxidation process.

## 2. EXPERIMENT

### 2.1. Synthesis of BDD and Pt NPs/BDD electrodes

Prior the experiment, fused silica glass(Shenyang Ebetter Optics Co., Ltd., China) as substrate was polished with slurry polishing powder (5-10  $\mu\text{m}$ , Zhengzhou Best Synthetic Diamond Co. Ltd., China) and was ultrasonically cleaned in acetone(99%,Xilong Scientific Co., Ltd., China) for 5 minutes and ethanol (99%,Shandong S-Sailing Chemical Co., Ltd., China) for 10 minutes, respectively. in order to hydrogenation of substrate in the plasma to develop the diamond seeding efficiency, the cleaned and dried fused silica glass transferred to stainless-steel vacuum chamber (CY-PECVD-T01, Zhengzhou CY Scientific Instrument Co., Ltd., China) at room temperature with 1200 W for 1 hour and hydrogen flow 60 sccm and pressure 65 Pa.

The BDD electrode was grown in microwave plasma assisted chemical vapor deposition system (MWCVD, SEKI Technotron AX5400S, Japan) from a 3 %  $\text{CH}_4$  solution in  $\text{H}_2$  with flow rate of 350 sccm and pressure of  $10^{-4}$  pa at 450 °C under excited plasma (3 GHz) and power of 1300 W for 1 hour. The doping of boron was conducted from the diborane in the gas phase (4000 ppm) which was injected into the MWCVD chamber.

Electrochemical deposition of Pt nanoparticles on prepared BDD electrode was carried out in three-electrode electrochemical cell contained 3 M Ag/AgCl as reference electrode, Pt as counter electrode and BDD electrode as working electrodes in 2 M Chloroplatinic Acid Hexahydrate (99%,

Shanghai Theorem Chemical Technology Co., Ltd., China) electrolyte. All electrochemical measurement and deposition were conducted on potentiostat/galvanostat Methrom Autolab (PGSTAT 30, Utrecht, The Netherlands).

## 2.2. Characterization and measurements

The scanning electron microscopy (SEM, Zeiss Supra-40) was applied to study the morphology of surface of prepared electrodes. X-ray diffraction (XRD, Philips PW3040/60/PANalyticalX'Pert Pro-MPD Powder Diffractometer with Cu  $K_{\alpha}$  radiation ( $\lambda = 0.154$  nm) was used for characterizations of crystal structures of prepared electrodes. Raman analysis was carried out in a confocal microRaman system (LabRAM ARAMIS, Horiba JobinYvon, France). Cyclic voltammetry (CV) analysis was conducted on electrochemical system in 0.5 M  $H_2SO_4$  (98%, Huaqiang Chemical Group Stock Co. Ltd., China) solution and 0.1 M tetrabutylammonium perchlorate (TBAP, 99%, Shanghai Smart Chemicals Co., Ltd., China) in 0.1 M dimethyl sulfoxide (DMSO,  $\geq 99.90\%$ , Haihang Industry Co., Ltd., China) with volume ratio of 1:1 as a base electrolyte.

The used leachate concentrates were obtained from a municipal landfill located in Guangzhou city, China. The leachate concentrates had been treated in nitrification process with air micro-bubble aeration tank in sequencing batch reactor. The amount of air entering the reactor was automatically adjusted to a stable set-point at  $0.9 O_2$  mg  $l^{-1}$ , and denitrification process with acetic acid (90%, Xilong Scientific Co., Ltd., China) by a membrane dosing pump, and treated biochemical system under ultrafiltration and nanofiltration membranes (LX-300K, Synder Filtration, Vacaville, CA), respectively. Physical and chemical properties were analyzed according to standard methods for the examination of water and wastewater (APHA)[14]: pH, conductivity (by a portable multiparameter HL-HQ40d multi, HACH, Germany); nitrogen compounds, total phosphorus, COD using a spectrophotometer (Hach / Dr Lange Modell: XION 500, LPG385, GmbH, Germany); 5-day biochemical oxygen demand ( $BOD_5$ ) using the manometric respirometry method (OxiTop® system, WTW, Weilheim, Germany)[15]. Colour measurements were performed according to the Pt-Co standard method [14]. The properties of used landfill leachate are shown in Table 1. The electrochemical oxidation experiments was conducted on cylindrically Plexiglas batch reactor under galvanostatic condition for treatment of 200 ml landfill leachate which filtered using a PTFE (2-6  $\mu m$ , Qingdao Yuan Dong Flon New Materials Co. Ltd., China) and pumped into the reactor and continuously recirculated for 7 hours at a flow rate of 5.5  $Lh^{-1}$ . The prepared electrodes (BDD and Pt NPs/BDD) as anodes and a 316 AISI stainless steel as cathode with areas of  $30 cm^2$  were placed vertically parallel to each other. The inter-electrode gap was kept constant 3 cm. electrochemical oxidation was carried out under galvanostatic condition powered by DC power supply (Testronix 34d, 0-15V and 0-10A) and current-voltage monitoring. The electrolyte was magnetically stirred during the experiment.

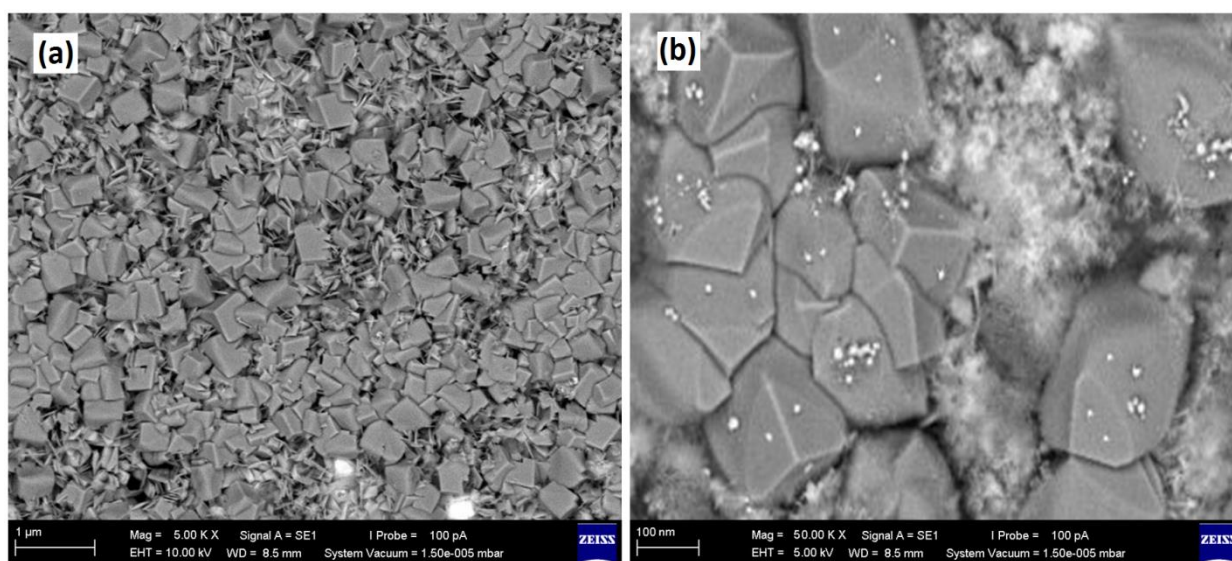
**Table 1.** Physical and chemical properties of used leachate in this study (mean  $\pm$  standard deviation (SD))

Property	Mean value $\pm$ SD (mg l <sup>-1</sup> )
COD	4002.11 $\pm$ 13.12
BOD <sub>5</sub>	198.98 $\pm$ 22.14
Nitrogencompounds	750.10 $\pm$ 21.25
Colour	247.44 $\pm$ 44.21
phosphorus	74.81 $\pm$ 11.27
pH	6.01 $\pm$ 0.01
conductivity	12.4 $\pm$ 0.1 mS cm <sup>-1</sup>

### 3. RESULTS AND DISCUSSION

#### 3.1. Structural characterization

The SEM images of the BDD and Pt NPs/BDD electrodes are shown in Figure 1. As observed, the homogeneous and dense diamond crystals covered the electrodes surface. The surface is without forming cracks or pinholes. The average of diamond grains are about 236 nm for both BDD electrodes. Moreover, there are parallel oriented ridges and grooves for both of electrodes which might refer to twin characteristics because of the nucleation in boron doping process [16]. For Pt NPs/BDD electrodes, Pt nanoparticles are scattered over the BDD surface which is assigned to a higher aspect ratio and porosity of Pt NPs/BDD surface toward BDD electrode surface.

**Figure 1.** SEM images of the (a) BDD and (b) Pt NPs/BDD electrodes.

XRD patterns of the BDD and Pt NPs/BDD electrodes are displayed in Figure 2. Two intense peaks are observed at  $2\theta = 43.31^\circ$  and  $75.69^\circ$  which are attributed to formation of the (111) and (220) planes of diamond, respectively in both electrodes according to diamond JCPDS Card No.06-0675[17]. For Pt NPs/BDD electrode two peaks at  $2\theta = 39.69^\circ$  and  $46.47^\circ$  are associated with (111) and (200) planes of Pt, respectively which evidence to formation of Pt in face-centered cubic (fcc) crystal phase according to Pt JCPDS Card No.04-0802[18]. Accordingly, Pt nanoparticles have been activated on the BDD electrode surface through electrodeposition method.

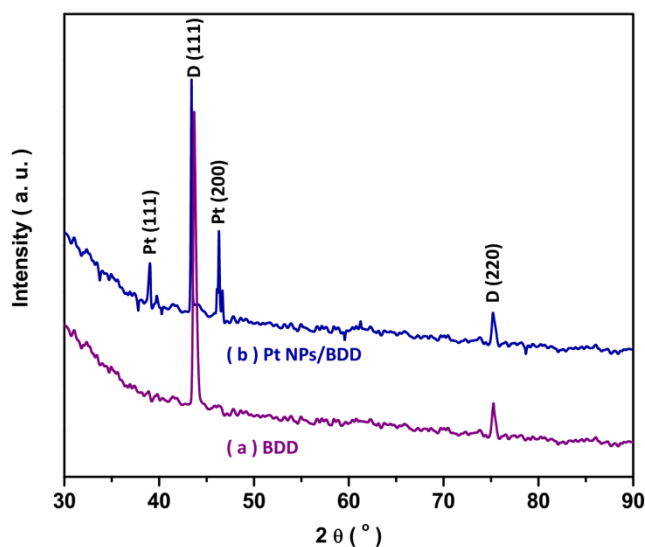


**Figure 2.** XRD patterns of the (a) BDD and (b) Pt NPs/BDD electrodes.

Figure 3 shows the Raman spectra of BDD and Pt NPs/BDD electrodes. The spectrum of BDD (Figure 3a) electrode presents a sharp peak at  $1334.3\text{ cm}^{-1}$  as diamond line with a FWHM of  $7.1\text{ cm}^{-1}$  which attributed to scattering from non-diamond carbon impurities such as defective  $sp^3$  hybridized graphitic carbon or surface impurities of amorphous carbon structure with mixture of  $sp^2$  and  $sp^3$  hybridization [19]. As observed, there is a peak at  $1588.1\text{ cm}^{-1}$  which is also assigned to scattering from defective graphitic carbon networks.

The spectrum of Pt NPs/BDD film (Figure 3b) exhibits a sharp peak at  $1337.1\text{ cm}^{-1}$  because phonon contributed to first-order Raman scattering. Raman peak position is shifted  $6\text{ cm}^{-1}$  toward higher frequency because of the intrinsic stress which formed by considerable difference in thermal expansion coefficients of diamond and Pt particles [20, 21]. The position and intensity of first-order diamond Raman peak depend on the internal stress, quality and crystallite size of film [22]. The positive shift of the Raman diamond line from the phase-pure diamond ( $1332.5\text{ cm}^{-1}$ ) could be evidence of presence of relative residual stress in Pt NPs/BDD film [22, 23]. Moreover, the full width at half maximum (FWHM) of the peak is obtained  $8.9\text{ cm}^{-1}$  which is higher value than the calculated value of high-quality single crystal diamond ( $2.1\text{ to }3\text{ cm}^{-1}$ ) [24]. The larger FWHM of Pt NPs/BDD film for the diamond line shows a higher degree of lattice imperfections because of the incorporated Pt particles. Furthermore, the observed low intense peak at  $1589\text{ cm}^{-1}$  in spectra of Pt NPs/BDD is related to

scattering of nondiamond impurity which might be attributed to formed no diamond impurities in the metal/diamond interface [25].

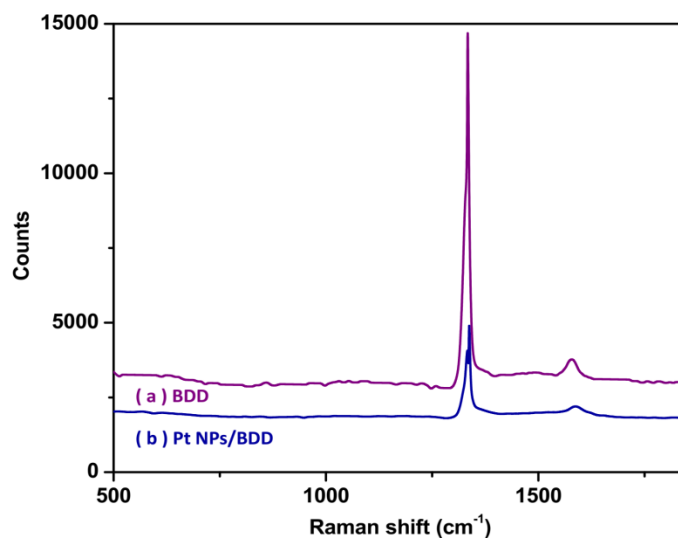
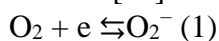


**Figure 3.** Raman spectra of the (a) BDD and (b) Pt NPs/BDD electrodes.

### 3.2. Electrochemical characterization

The recorded CVs of BDD and Pt NPs/BDD in 0.5 M H<sub>2</sub>SO<sub>4</sub> solution pH 2 at potential range -1.2 V to 2.2 V at scan rate 10 mVs<sup>-1</sup> is shown in Figure 4. As seen, the recorded background current of CVs are very close to zero in a wide range of applied potential. This lower current of Pt NPs/BDD can promote the degradation efficiency of organic pollutants because of a greater decrease of energy consumption in resistance of electrolyte and electrode interface [26]. The current oxygen evolution reaction is observed at high potential (>2 V). High evolution overpotential of oxygen can warrant the electrochemical oxidation of the main part of organic wastes with high current efficiency because of minimizing side reactions [27]. Furthermore, the high overpotential of oxygen evolution can be beneficial for the electrochemical incineration of organic species due to electro-generation and accumulation of oxidants such as hydroxyl radicals on electrodes[28]. Therefore, electrochemical characterization of Pt NPs/BDD electrode illustrates that it can be favorable material for leachate treatment.

The electrochemical response of COD was investigated by using BDD and Pt NPs/BDD electrodes in 0.1 M DMSO/TBAP solution through the record of CVs based on the reduction processes of molecular oxygen at electrodes surface under potential range -1.0 V to 0.5 V at scan rate of 20 mVs<sup>-1</sup> (Figure 5). It has been approved that in aprotic solvents the reduction of molecular oxygen to superoxide ion (O<sub>2</sub><sup>-</sup>) occurs under reversible one-electron process according to the following reaction[29]:



As seen from Figure 5 for BDD electrode in DMSO, the reduction of  $O_2$  to  $O_2^-$  took place at a potential of  $-0.57$  V, and the consequential re-oxidation of  $O_2^-$  to  $O_2$  occurred at a potential of  $0.02$  V. It is observed that the recorded redox current at Pt NPs/BDD electrode in DMSO/TBAP solution are higher peak currents than at BDD electrode. For Pt NPs/BDD electrode, the cathodic reduction peak is also observed at  $-0.57$  V, while the subsequent anodic re-oxidation peak is appeared at  $-0.14$  V. Another peak at  $0.17$  V is also observed in anodic process which implied to electro-oxidation of superoxide anion at Pt NPs/BDD electrode is complex and that the superoxide anion products are strongly adsorbed on the surface of Pt NPs/BDD electrode is quasi-reversible. Therefore, the electrode surface properties and morphology can effect on complex mechanism of redox reaction between the oxygen to superoxide ion through effect on thermodynamics and kinetics of reactions [30].

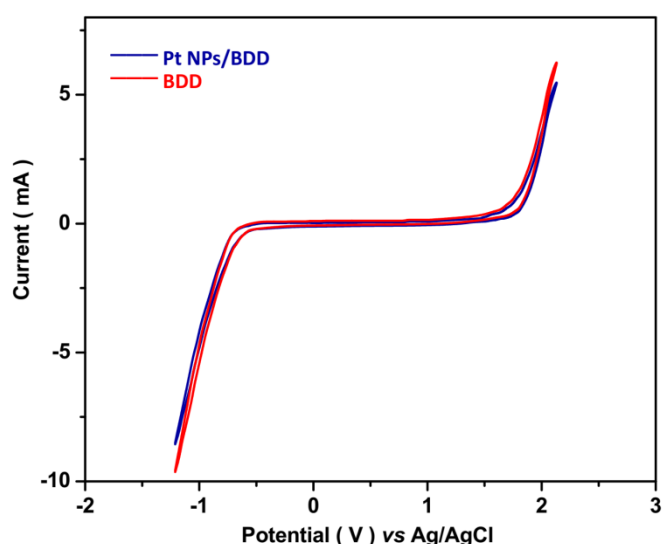


**Figure 4.** The recorded CVs of BDD and Pt NPs/BDD in 0.5 M  $H_2SO_4$  solution pH 2 at potential range  $-1.2$  V to  $2.2$  V at scan rate  $20$   $mVs^{-1}$

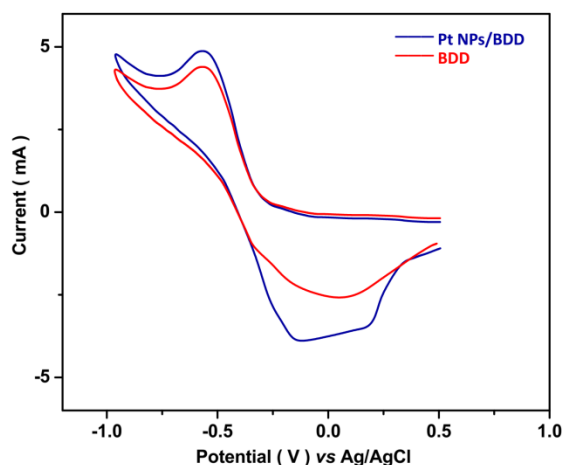


**Figure 5.** The recorded CVs of BDD and Pt NPs/BDD in 0.1 M DMSO/TBAP solution pH 3 at potential range  $-1.0$  V to  $0.5$  V at scan rate  $20$   $mVs^{-1}$

### 3.3. Study the electrochemical oxidation of COD

The direct electron transfer from organic compounds to the anode and generation of effective oxidant at the BDD based electrode can be in charge of the improved degradation of organic matters in an aquatic solution. The ability to generate the oxidants depends on the applied current density and the properties of anode material which indicated under low current density the system reaches a balance situation later [31-33]. In other words, under applied higher current densities, time of the reaction also shortens and energy consumption increases [31-34]. Therefore, the following experiments were investigated using current densities of 15, 50 and 100 mA cm<sup>-2</sup> similar to the previous reports [35-40].

The electrochemical oxidation of COD on BDD and Pt NPs/BDD was studied under different current densities of 15, 50 and 100 mA cm<sup>-2</sup> at pH 6 and flow velocity of 5.5 L h<sup>-1</sup>. Figure 6 shows that the removal of COD is performed with a higher rate within the first 3.5 hours and it continues with a slower rate in the last 2 hours for all applied current densities. The prepared BDD and Pt NPs/BDD have high efficiency at the initial hours of the treatment due to more superficial activated sites on electrodes. In the last hours of the treatment, the adsorbent sites on electrodes are saturated by pollutants. Figure 6a shows the COD has decreased about 67.8 %, 69.0 % and 71.8 % on BDD in current densities of 15, 50 and 100 mA cm<sup>-2</sup>, respectively, after 5.5 hours of electrochemical oxidation treatment. For sample Pt NPs/BDD in Figure 6b, the COD is decreased about 76.4 %, 84.3 % and 91.9 % for current densities of 15, 50 and 100 mA cm<sup>-2</sup>, respectively, after 5.5 hours treatment. For both electrodes, removal of COD is increased with increasing the applied current density. For higher applied current density (100 mA cm<sup>-2</sup>), the electron transfer rate is significantly increased and enhances the direct electrochemical oxidation of organic compounds [41].

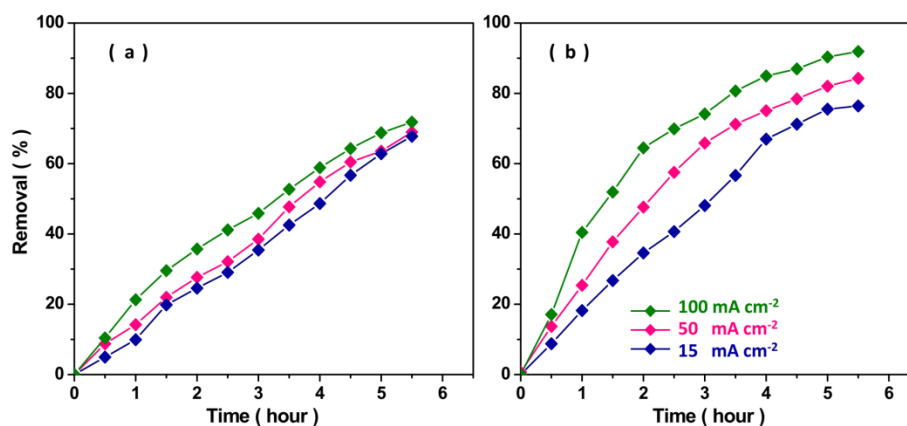


**Figure 6.** The electrochemical oxidation of COD on (a) BDD and (b) Pt NPs/BDD under different current densities of 15, 50 and 100 mA cm<sup>-2</sup> at pH 6 and flow velocity of 5.5 Lh<sup>-1</sup>.

In addition, the concentration of hydroxyl radicals has also been increased due to enhancement of water discharge rate which can be useful for indirect electrochemical oxidation of organic pollutants [42]. Results show that Pt NPs/BDD has the most efficiency to remove COD by electrochemical

oxidation process. Pt nanoparticles on BDD could promote the electrochemical oxidation rate of organic pollutants through the enhancement of the physically adsorbed hydroxyl radicals and chemisorbed oxygen in metal lattice [43]. Therefore, there are more oxidation states on the active surface of Pt NPs/BDD electrode and more adsorbed hydroxyl radicals interact with the BDD surfaces [42, 43]. Studies showed that the chemical structure of BDD makes it desirable for remove the colour and organic pollutants because of cleavage in different parts of dye [44, 45]. It suggested that the boron doping level in diamond influences on ratio of  $sp^2/sp^3$  which could be effective to degradation of organic compounds [2]. Studies on Pt anodes shows this anode is appropriate to 100 % oxidation of colour through breaking azo bands of dye [46]. It have been reported that Pt electrode favours to oxidation of large variety of different bio-refractory organic substances such that during removal process, aromatic molecules are adsorbed on Pt electrode and lead to formation of aromatic intermediates, subsequently the ring of aromatic intermediates are opened [46, 47]. Therefore, Pt NPs/BDD in this study provides the synergetic effect of BDD and Pt advantages to electrochemical oxidation of COD. In accordance to SEM images, Pt NPs/BDD electrode, scattered Pt nanoparticles on Pt NPs/BDD electrode surface show the higher aspect ratio and more porous structure than BDD electrode which be beneficial to more physically adsorbed and chemisorbed active species to treatment [48-50]. Therefore, the following study was conducted on Pt NPs/BDD electrode.

Energy consuming ( $E_c$ ) and instantaneous current efficiency (ICE) are important parameters for electrochemical oxidation treatment of leachate that determine the efficiency and cost of the process.  $E_c$  ( $kWh \cdot m^{-3}$ ) and ICE (%) are estimated using the equation (2) and (3), respectively [51]:

$$E_c = \frac{UIt}{60V} \quad (2)$$

$$ICE = \frac{(COD_0 - COD_t)FV}{8It} \quad (3)$$

Where U (V), I (A), t (minute) and V (l) are the mean applied voltage, current, the time of treatment and the volume of electrolyte, respectively. In equation (3),  $COD_0$  ( $g l^{-1}$ ) and  $COD_t$  ( $g l^{-1}$ ) are the chemical oxygen demands before electrochemical oxidation treatment and at time t, respectively. F ( $96487 \text{ C mol}^{-1}$ ) is the Faraday constant. Figure 7 shows the calculated ICE values for different current densities. It illustrates that ICE value is 88.02% after one hour of treatment, then it gradually decrease to 64.98% after 5.5 hours treatment under  $15 \text{ mA cm}^{-2}$  of current density which can be associated with the adsorption of the organic substances on the electrode surface that it prevents the direct electron transfer between the electrode surface and organic species [51]. The similar results of decreasing of ICE are observed for both of current densities of 50 and  $100 \text{ mA} \cdot \text{cm}^{-2}$ .

Figure 8 displays the  $E_c$  and ICE values after 5.5 hours electrochemical oxidation under different current densities of 15, 50 and  $100 \text{ mA cm}^{-2}$  at pH 6 and flow velocity of  $5.5 \text{ L h}^{-1}$ . As seen,  $E_c$  value for 5.5 hours treatment under current density of  $50 \text{ mA} \cdot \text{cm}^{-2}$  ( $215.4 \text{ kWh m}^{-3}$ ) is remarkably lower than the obtained value under  $100 \text{ mA} \cdot \text{cm}^{-2}$  ( $424.7 \text{ kWh m}^{-3}$ ). Beyond that the obtained ICE value at under  $100 \text{ mA} \cdot \text{cm}^{-2}$  is 18.5 % which is the lowest value between the applied current densities after 5.5 hours treatment. Therefore, the highest  $E_c$  and lowest ICE values are obtained under maximum current density that might be attributed to the increment of side reactions [52]. Furthermore, results indicate that the appropriate current density is  $50 \text{ mA cm}^{-2}$ .

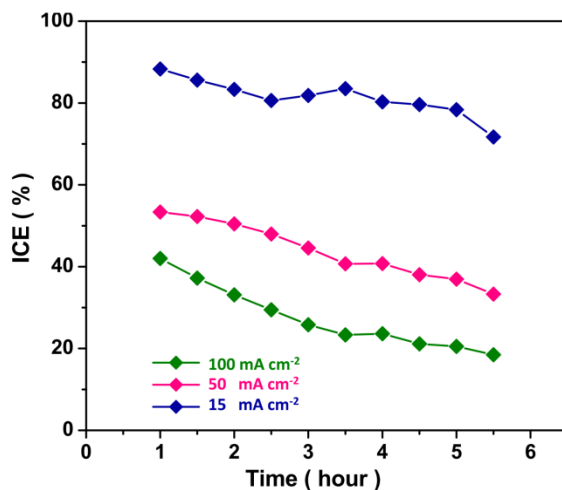


**Figure 7.** Obtained ICE values for landfill leachate treatment by electrochemical oxidation under different current densities of 15, 50 and 100 mA cm<sup>-2</sup> at pH 6 and flow velocity of 5.5 L h<sup>-1</sup>

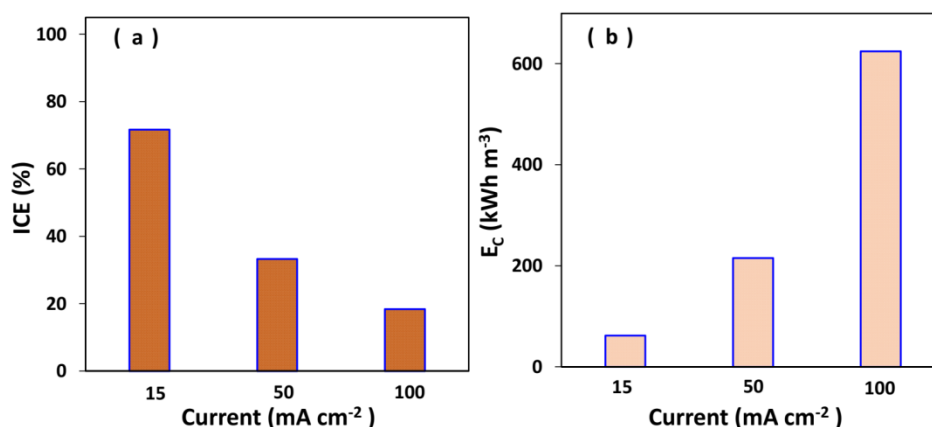


**Figure 8.** Obtained (a) E<sub>C</sub> and (b) ICE values for landfill leachate treatment after 5.5 h electrochemical oxidation under different current densities of 15, 50 and 100 mA cm<sup>-2</sup> at pH 6 and flow velocity of 5.5 L h<sup>-1</sup>

#### 4. CONCLUSION

In this paper, the treatment of municipal solid waste landfill leachate was studied using BDD and Pt NPs/BDD as anodes through the electrochemical oxidation process. The BDD anode was synthesized using MWCVD technique and then Pt nanoparticles were electrodeposited on prepared BDD electrodes. The structural and electrochemical properties of prepared BDD and Pt NPs/BDD anodes were analyzed. The SEM and XRD analyses showed that the homogeneous and dense diamond crystals covered the both electrodes surfaces and for Pt NPs/BDD electrodes, Pt nanoparticles in fcc crystal phase scattered over the BDD surface. Raman analysis indicated the presence of non-diamond carbon impurities and higher degree of lattice imperfections because of the incorporated Pt particles in

BDD and Pt NPs/BDD structures, respectively. The electrochemical oxidation of COD showed that COD was decreased about 67.8 %, 69.0 % and 71.8 % on BDD, and decreased about 76.4 %, 84.3 % and 91.9 % on Pt NPs/BDD for current densities of 15, 50 and 100 mA cm<sup>-2</sup>, respectively, after 5.5 hours treatment. Results show that Pt NPs/BDD revealed the most efficiency to treatment of COD by electrochemical oxidation process. Pt nanoparticles on BDD could develop the electrochemical oxidation rate of organic pollutants through the enhancement of the physically adsorbed hydroxyl radicals and chemisorbed oxygen in metal lattice. Therefore, Pt NPs/BDD electrodes have more oxidation states on the active surface and more adsorbed hydroxyl radicals which interact with the BDD surface. Pt NPs/BDD in this study provides the synergetic effect of BDD and Pt advantages to electrochemical oxidation of COD.

#### ACKNOWLEDGEMENT

This work was sponsored in part by high-level talent research project of North China University of Water Resources and Electric Power (201617).

#### References

1. H. Karimi-Maleh, Y. Orooji, A. Ayati, S. Qanbari, B. Tanhaei, F. Karimi, M. Alizadeh, J. Rouhi, L. Fu and M. Sillanpää, *Journal of Molecular Liquids*, (2020)115062.
2. M.D. Vaverková, J. Elbl, E. Koda, D. Adamcová, A. Bilgin, V. Lukas, A. Podlasek, A. Kintl, M. Wdowska and M. Brtnický, *Sustainability*, 12(2020)4531.
3. N. Ferronato and V. Torretta, *International journal of environmental research and public health*, 16(2019)1060.
4. J. Rouhi, S. Kakooei, S.M. Sadeghzadeh, O. Rouhi and R. Karimzadeh, *Journal of Solid State Electrochemistry*, 24(2020)1599.
5. I. Ilankoon, Y. Ghorbani, M.N. Chong, G. Herath, T. Moyo and J. Petersen, *Waste Management*, 82(2018)258.
6. J. Kanagaraj, T. Senthilvelan, R. Panda and S. Kavitha, *Journal of Cleaner Production*, 89(2015)1.
7. J. Rouhi, S. Kakooei, M.C. Ismail, R. Karimzadeh and M.R. Mahmood, *International Journal of Electrochemical Science*, 12(2017)9933.
8. S. Arslan, M. Eyvaz, E. Gürbulak and E. Yüksel, *Textile wastewater treatment*, 1(2016)1.
9. M. Afsharnia, H. Biglari, S.S. Rasouli, A. Karimi and M. Kianmehr, *International Journal of Electrochemical Science*, 13(2018)472.
10. Q. Feng, L. Xu, Y. Xu, C. Liu, Y. Lu, H. Wang, T. Wu, R. Wang, Y. Chen and Y. Cheng, *International Journal of Electrochemical Science*, 15(2020)1022.
11. G. Hassani, A. Alinejad, A. Sadat, A. Esmaeili, M. Ziaei, A.A. Bazrafshan and T. Sadat, *International Journal of Electrochemical Science*, 11(2016)6705.
12. H. Karimi-Maleh, M. Alizadeh, Y. Orooji, F. Karimi, M. Baghayeri, J. Rouhi, S. Tajik, H. Beitollahi, S. Agarwal and V.K. Gupta, *Industrial & Engineering Chemistry Research*, 60(2021)816.
13. M. Errami, R. Salghi, E.E. Ebenso, M. Messali, S. Al-Deyab and B. Hammouti, *International Journal of Electrochemical Science*, 9(2014)5467.
14. A.P.H. Association, A.W.W. Association, W.P.C. Federation and W.E. Federation, *Standard methods for the examination of water and wastewater*. Vol. 2. 1912: American Public Health Association.

15. E. Bazrafshan, H. Moein, F. Kord Mostafapour and S. Nakhaie, *Journal of Chemistry*, 2013(2013)640139.
16. V. Lebedev, T. Yoshikawa, C. Schreyvogel, L. Kirste, J. Weippert, M. Kunzer, A. Graff and O. Ambacher, *Journal of Applied Physics*, 127(2020)025303.
17. X. Liu, H. Wang, P. Lu, Y. Ren, X. Tan, S. Sun and H. Jia, *Coatings*, 8(2018)163.
18. M. Shah, *Scientia Iranica*, 19(2012)964.
19. R. Haerle, E. Riedo, A. Pasquarello and A. Baldereschi, *Physical Review B*, 65(2001)045101.
20. T. Tachibana, Y. Yokota, K. Miyata, T. Onishi, K. Kobashi, M. Tarutani, Y. Takai, R. Shimizu and Y. Shintani, *Physical Review B*, 56(1997)15967.
21. T. Tachibana, Y. Yokota, K. Kobashi and M. Yoshimoto, *Journal of crystal growth*, 205(1999)163.
22. G. Faggio, G. Messina, S. Santangelo, G. Prestopino, I. Ciancaglioni and M. Marinelli, *Journal of Quantitative Spectroscopy and Radiative Transfer*, 113(2012)2476.
23. A.F. Azevedo, E.J. Corat, N.F. Leite, N.G. Ferreira and V.J. Trava-Airoldi, *Materials Research*, 6(2003)51.
24. M. Donato, G. Faggio, M. Marinelli, G. Messina, E. Milani, A. Paoletti, S. Santangelo, A. Tucciarone and G.V. Rinati, *The European Physical Journal B-Condensed Matter and Complex Systems*, 20(2001)133.
25. J.-S. Gao, T. Arunagiri, J.-J. Chen, P. Goodwill, O. Chyan, J. Perez and D. Golden, *Chemistry of materials*, 12(2000)3495.
26. B. Thokchom, A.B. Pandit, P. Qiu, B. Park, J. Choi and J. Khim, *Ultrasonics Sonochemistry*, 27(2015)210.
27. F. Sharif and E.P. Roberts, *Catalysts*, 10(2020)263.
28. E. Nurhayati, *Jurnal Sains & Teknologi Lingkungan*, 4(2012)24.
29. D. Maricle and W. Hodgson, *Analytical Chemistry*, 37(1965)1562.
30. M. Hayyan, M.A. Hashim and I.M. AlNashef, *Chemical reviews*, 116(2016)3029.
31. Y. Jiang, H. Zhao, J. Liang, L. Yue, T. Li, Y. Luo, Q. Liu, S. Lu, A.M. Asiri and Z. Gong, *Electrochemistry Communications*, (2021)106912.
32. R. Niazmand, M. Jahani, F. Sabbagh and S. Rezaia, *Water*, 12(2020)1687.
33. S. Bayar, Y. Yildiz, A. Yilmaz and A.S. Koparal, *Desalination and Water Treatment*, 52(2014)3047.
34. E. Vaiopoulou, P. Melidis and A. Aivasidis, *Journal of hazardous materials*, 186(2011)1141.
35. N. Bensalah, S. Dbira, A. Bedoui and M.I. Ahmad, *Processes*, 8(2020)460.
36. F. Agustina, A. Bagastyo and E. Nurhayati, *Water Science and Technology*, 79(2019)921.
37. E. Hmani, Y. Samet and R. Abdelhédi, *Diamond and Related Materials*, 30(2012)1.
38. I. Jum'h, A. Abdelhay, A. Telfah, M.-A. Al-Akhras, A. Al-Kazwini and S. Rosiwal. *Veratric acid removal from water by electrochemical oxidation on BDD anode*. in *IOP Conference Series: Materials Science and Engineering*. 2018: IOP Publishing.
39. M.B. Brahim, H.B. Ammar, R. Abdelhédi and Y. Samet, *Korean Journal of Chemical Engineering*, 33(2016)2602.
40. C. Wang, J. Wang, X. Ma, H. Li and S. Zhang, *Journal of Chemistry*, 2015(2015)617850.
41. C.A. Martínez-Huitle and S. Ferro, *Chemical Society Reviews*, 35(2006)1324.
42. Y. He, H. Lin, Z. Guo, W. Zhang, H. Li and W. Huang, *Separation and Purification Technology*, 212(2019)802.
43. C.A. Martínez-Huitle and L.S. Andrade, *Quimica Nova*, 34(2011)850.
44. H. Akrouf and L. Bousselmi, *Arabian Journal of Geosciences*, 6(2013)5033.
45. H. Karimi-Maleh, S. Ranjbari, B. Tanhaei, A. Ayati, Y. Orooji, M. Alizadeh, F. Karimi, S. Salmanpour, J. Rouhi and M. Sillanpää, *Environmental Research*, 195(2021)110809.
46. J. Florêncio, M. Pacheco, A. Lopes and L. Ciríaco, *Portugaliae Electrochimica Acta*, 31(2013)257.

47. C.A. Martínez-Huitle, M.A. Rodrigo, I. Sirés and O. Scialdone, *Chemical Reviews*, 115(2015)
48. F. Chahshouri, H. Savaloni, E. Khani and R. Savari, *Journal of Micromechanics and Microengineering*, 30(2020)075001.
49. N. Kostoglou, C.-W. Liao, C.-Y. Wang, J.N. Kondo, C. Tampaxis, T. Steriotis, K. Giannakopoulos, A.G. Kontos, S. Hinder and M. Baker, *Carbon*, 171(2020)294.
50. H. Savaloni, R. Savari and S. Abbasi, *Current Applied Physics*, 18(2018)869.
51. F. Hachami, M. Errami, L. Bazzi, M. Hilali, R. Salghi, S. Jodeh, B. Hammouti and O.A. Hamed, *Chemistry Central Journal*, 9(2015)1.
52. D. Myburgh, M. Aziz, F. Roman, J. Jardim and S. Chakawa, *Environmental Processes*, 6(2019)819.

© 2021 The Authors. Published by ESG ([www.electrochemsci.org](http://www.electrochemsci.org)). This article is an open access article distributed under the terms and conditions of the Creative Commons Attribution license (<http://creativecommons.org/licenses/by/4.0/>).